Available online at www.sciencedirect.com
ScienceDirect
Geochimica et Cosmochimica Acta 71 (2007) 1385–1397
Geochimica et Cosmochimica Acta
www.elsevier.com/locate/gca

Field experiments yield new insights into gas exchange and excess air formation in natural porous media

Stephan Klump [a,b,*], Yama Tomonaga [a], Peter Kienzler [c], Wolfgang Kinzelbach [c], Thomas Baumann [d], Dieter M. Imboden [b], Rolf Kipfer [a,e]

[a] *Eawag, Swiss Federal Institute of Aquatic Science and Technology, 8600 Dübendorf, Switzerland*
[b] *Institute of Biogeochemistry and Pollutant Dynamics, ETH Zurich, 8092 Zurich, Switzerland*
[c] *Institute of Environmental Engineering, ETH Zurich, 8092 Zurich, Switzerland*
[d] *Institute of Hydrochemistry, TU München, 81377 Munich, Germany*
[e] *Institute of Isotope Geochemistry and Mineral Resources, ETH Zurich, 8092 Zurich, Switzerland*

Received 24 May 2006; accepted in revised form 13 December 2006; available online 19 December 2006

Abstract

Gas exchange between seepage water and soil air within the unsaturated and quasi-saturated zones is fundamentally different from gas exchange between water and gas across a free boundary layer, e.g., in lakes or rivers. In addition to the atmospheric equilibrium fraction, most groundwater samples contain an excess of dissolved atmospheric gases which is called "excess air". Excess air in groundwater is not only of crucial importance for the interpretation of gaseous environmental tracer data, but also for other aspects of groundwater hydrology, e.g., for oxygen availability in bio-remediation and in connection with changes in transport dynamics caused by the presence of entrapped air bubbles. Whereas atmospheric solubility equilibrium is controlled mainly by local soil temperature, the excess air component is characterized by the (hydrostatic) pressure acting on entrapped air bubbles within the quasi-saturated zone. Here we present the results of preliminary field experiments in which we investigated gas exchange and excess air formation in natural porous media. The experimental data suggest that the formation of excess air depends significantly on soil properties and on infiltration mechanisms. Excess air was produced by the partial dissolution of entrapped air bubbles during a sprinkling experiment in fine-grained sediments, whereas similar experiments conducted in coarse sand and gravel did not lead to the formation of excess air in the infiltrating water. Furthermore, the experiments revealed that the noble gas temperatures determined from noble gases dissolved in seepage water at different depths are identical to the corresponding in situ soil temperatures. This finding is important for all applications of noble gases as a paleotemperature indicator in groundwater since these applications are always based on the assumption that the noble gas temperature is identical to the (past) soil temperature.

1. INTRODUCTION

Atmospheric gases are incorporated into groundwater by gas exchange between seepage water and soil air during infiltration. The atmospheric solubility equilibrium is controlled by soil temperature and atmospheric pressure. However, the concentrations of atmospheric gases dissolved in groundwater are usually found to exceed their respective atmospheric equilibrium concentrations. Because the composition of the excess gas fraction is often similar to that of atmospheric air, Heaton and Vogel (1981) introduced the term "excess air" for this characteristic excess gas component of groundwater. Since the first observation of Ar supersaturation in Japanese aquifers (Oana, 1957), excess air in groundwater has been reported in numerous groundwater studies under different climatic and hydrogeological conditions, including studies in different climatic regions and on different aquifer types as well as studies on both

* Corresponding author.
E-mail address: stephan.klump@eawag.ch (S. Klump).

0016-7037/$ - see front matter © 2006 Elsevier Inc. All rights reserved.
doi:10.1016/j.gca.2006.12.006

young and old groundwaters (Mazor, 1972; Stute et al., 1995b; Wilson and McNeill, 1997; Aeschbach-Hertig et al., 1999, 2000; Kipfer et al., 2002). Thus, the presence of excess air is now known to be a fundamental property of almost all kinds of groundwater.

A widely accepted conceptual model of excess air formation is the partial dissolution of entrapped air bubbles within the quasi-saturated zone (Heaton and Vogel, 1981; Holocher et al., 2002, 2003). Due either to a rising groundwater table or to the formation of quasi-saturated lenses within the unsaturated zone during the infiltration process, the water phase does not completely remove the gas phase from the pore space of the soil matrix. Instead, air bubbles are entrapped by the surrounding water phase and are exposed to an increased hydrostatic pressure. As a result, the local solubility equilibrium exceeds that of the free atmosphere, and hence the air bubbles are forced to dissolve partly or completely in the water phase, depending on the degree of local pressure enhancement.

Excess air and its formation are of great importance in subsurface hydrology. Atmospheric trace gases – e.g., the noble gases, sulfur hexafluoride, and chlorofluorocarbons – are used as environmental tracers for investigating physical processes in groundwater, for reconstructing environmental conditions in the past, and for dating purposes (Cook and Herczeg, 2000; Kipfer et al., 2002). Most applications of gaseous environmental tracers require separation of the excess air component from the atmospheric equilibrium fraction. This is needed to interpret the tracer data in terms of the environmental conditions prevailing during water infiltration. In order to reliably identify and separate out the excess air component, different lumped-parameter models have been developed that are commonly used to correct noble gas concentrations of groundwater samples for the excess air component (Kipfer et al., 2002). These simplistic excess air models are clearly limited in a strict physical sense, and yield a parameterization of the excess air rather than a mechanistic description of the processes controlling its formation.

Although the phenomenon of excess air in groundwater has been known for decades, a sound physical description of its formation in natural aquifer systems is still lacking. Recently, Holocher et al. (2003) developed the Kinetic Bubble Dissolution (KBD) model, which gives a mechanistic description of the dissolution of entrapped air bubbles in quasi-saturated porous media based on physical principles. In addition, Holocher et al. (2002) were able to produce excess air in sand column experiments, the results of which were in accordance with the predictions of the KBD model and with observations in the field. These experiments confirm the validity of the conceptual model of the dissolution of entrapped air bubbles on the laboratory scale and yield some insight into the real physical processes that govern air/water partitioning within the quasi-saturated zone and which are parameterized by the lumped-parameter models. However, the validation of the concepts which describe the formation of excess air under natural conditions has up to now been addressed only poorly.

In this paper, we present the results of two field experiments conducted under different hydrological conditions to assess gas exchange and the formation of excess air in quasi-saturated soils under natural conditions, using dissolved noble gases as conservative tracers. We focused mainly on soil temperature and air entrapment, as these factors are presumed to exert a crucial control on gas exchange and excess air formation during infiltration.

2. THEORY

2.1. Noble gases as environmental tracers

Noble gases are widely used as environmental tracers in subsurface hydrology. Atmospheric (noble) gases are incorporated into groundwater by gas exchange between rainwater and atmosphere, and between seepage water and soil air during infiltration. As soon as the water enters the saturated zone, no further gas exchange occurs. Since noble gases are chemically inert, the groundwater maintains the dissolved noble gas concentrations as a marker of the physical conditions (temperature, pressure, salinity) that prevailed during the infiltration process. This allows past climatic conditions to be reconstructed from atmospheric noble gases dissolved in groundwater (Mazor, 1972; Stute et al., 1995a,b; Beyerle et al., 1998, 1999, 2003; Aeschbach-Hertig et al., 2000).

The noble gas temperature (NGT), which can be derived from the dissolved noble gas concentrations, is defined by the temperature that prevailed during the last gas exchange between the groundwater and the atmosphere. Since the last gas exchange usually occurs close to the groundwater table during infiltration, the NGT is assumed to be identical to the soil temperature prevailing during groundwater recharge (Stute and Sonntag, 1992; Stute and Schlosser, 1993). The soil temperature is a crucial factor controlling the gas exchange between seepage water and soil air. Numerous paleoclimate studies have been conducted using noble gases to determine past soil temperatures (reviewed by Kipfer et al. (2002)). All these studies rely on the assumption that the NGT is equal to the mean annual soil temperature. The field experiments carried out gave us the opportunity to assess the validity of this assumption in addition to conducting the study on excess air formation.

2.2. Gas exchange in porous media

Atmospheric gases are incorporated into groundwater as a result of gas exchange between the water and the atmosphere or soil air. The dissolution of atmospheric (noble) gases in natural waters can be described according to Henry's Law:

$$C_i^{\mathrm{equ}} = \frac{C_i^{\mathrm{atm}}}{K_{\mathrm{H},i}(T,S)} = \frac{P_i}{R \cdot T \cdot K_{\mathrm{H},i}(T,S)} \quad (1)$$

The equilibrium concentration C_i^{equ} of the dissolved gas i is directly proportional to its local atmospheric concentration C_i^{atm}. Dalton's Law, in which R is the universal gas constant, relates the molar atmospheric concentration of gas i to its partial pressure P_i in the gas phase. The concentration proportionality is given by the nondimensional Henry coefficient $K_{\mathrm{H},i}$, the value of which depends on the physical

conditions (e.g., temperature T and salinity S) prevailing during gas partitioning.

The solubilities of the noble gases increase with atomic mass from He to Xe (Weiss, 1970, 1971; Weiss and Kyser, 1978; Clever, 1979). The strongly temperature dependent solubilities of the heavy noble gases Ar, Kr, and Xe allow the temperature that prevailed during infiltration to be reconstructed. The least soluble light noble gases He and Ne react most sensitively to the presence of excess air, and they are therefore used to quantify the excess air component in groundwater samples. However, most groundwaters contain terrigenic He in addition to atmospheric He, and therefore Ne, which is of atmospheric origin only, is commonly used to determine the excess air component in groundwaters. Excess air is therefore often expressed in terms of relative Ne supersaturation (ΔNe); i.e., the Ne excess ($C_{\mathrm{Ne}}^{\mathrm{exc}}$) as a percentage of its atmospheric equilibrium concentration ($C_{\mathrm{Ne}}^{\mathrm{equ}}$).

$$\Delta\mathrm{Ne} = \frac{C_{\mathrm{Ne}}^{\mathrm{exc}}}{C_{\mathrm{Ne}}^{\mathrm{equ}}} \cdot 100(\%) \tag{2}$$

Whereas solubility increases with atomic mass, molecular diffusivity decreases. Hence, the light noble gases He and Ne react more sensitively to any diffusive alterations in the dissolved noble gas concentrations than do the heavier noble gases Ar, Kr and Xe.

2.2.1. Kinetic bubble dissolution (KBD) model

Holocher et al. (2003) developed the KBD model to describe the dissolution of entrapped air bubbles in quasi-saturated porous media. The bubbles are assumed to consist of the noble gases He, Ne, Ar, Kr, Xe, and the two main air constituents N_2 and O_2. The mass transfer between the spherical air bubbles and the water phase is modeled by assuming rapid local equilibration between the air bubbles and the surrounding water phase according to Henry's Law (Eq. (1)) and by making use of a water-side boundary layer gas exchange approach (e.g., Schwarzenbach et al., 2003). The local pressure in the air bubbles has to be equal to the local total pressure, which is the sum of atmospheric, hydrostatic, and surface-tension pressures, the latter being the result of the curvature of the bubble surface. In the case of flowing groundwater, the compositions of the gas and water phases change due to dissolution and due to the differing Henry coefficients of the gases, and the volumes of the gas bubbles shrink with time. As a result, gases from the gas phase are transferred to the water phase, yielding a typical excess air signal in the groundwater. Given the hydrological settings as boundary conditions, the KBD model was able to reproduce the amount as well as the elemental fractionation of excess air in laboratory experiments (Holocher et al., 2002). For a more detailed description of the KBD model, see Holocher et al. (2003).

2.2.2. Lumped-parameter models

For practical purposes, including the interpretation of dissolved noble gases in groundwater, simplified lumped-parameter models are commonly used for the parameterization of the amount of excess air in order to separate the measured gas concentrations into equilibrium and excess air components. Several conceptual excess air models have been developed. The simplest model assumes the excess air component to be unfractionated with respect to atmospheric air (Heaton and Vogel, 1981), whereas other models presume fractionated excess air (e.g., partial re-equilibration model, Stute et al., 1995b; closed-system equilibration model, Aeschbach-Hertig et al., 2000; capillary pressure model, Mercury et al., 2004).

According to the closed-system equilibration (CE) model, the formation of excess air is the result of the equilibration of a finite water volume with a finite air volume at increased hydrostatic pressure within the quasi-saturated zone:

$$C_i(T,S,P_{\mathrm{atm}},A,F) = C_i^{\mathrm{equ}}(T,S,P) + \frac{(1-F)\cdot A\cdot z_i}{1+F\cdot A\cdot z_i/C_i^{\mathrm{equ}}(T,S,P)} \tag{3}$$

The initial amount of entrapped air is given by A, whereas the fractionation parameter F describes the reduction of this initial gas volume due to dissolution and compression. The parameter z_i is the volume fraction of gas i in dry air.

If the entire volume of entrapped air is completely dissolved, the result is pure, unfractionated excess air. If the hydrostatic pressure is not sufficient for complete dissolution, the composition of both the dissolved gas and the remaining gas phase is fractionated; i.e., the elemental composition is fractionated relative to pure atmospheric air, whereas there is hardly any effect on the isotopic composition of any given element (e.g., Kipfer et al., 2002). Due to their high solubilities, the heavy noble gases Ar, Kr and Xe are enriched in the water phase relative to the poorly soluble, light noble gases He and Ne.

The degree of fractionation of the excess air component is described by the fractionation factor F:

$$F = \frac{V}{Q} \tag{4}$$

where $V = V_{\mathrm{g}}/V_{\mathrm{g}}^0$ is the ratio of the volume of entrapped air in the final state (V_{g}) to that in the initial state (V_{g}^0), and $Q = (P_{\mathrm{tot}} - e_{\mathrm{w}})/(P - e_{\mathrm{w}})$ is the ratio of the dry gas pressure in the entrapped gas (P_{tot}) to that in the free atmosphere (P), with e_{w} being the saturation water vapor pressure. Typically, more air is entrapped in the soil matrix than can be dissolved at the prevailing pressure. Fractionation of the resulting excess air component is therefore similar to that described by the CE model, and its size, expressed as ΔNe (Eq. (2)), is limited by the pressure acting on the entrapped air bubbles. The fractionation factor F ranges from 0 to 1; i.e., $F = 0$ implies complete dissolution of the entrapped air bubbles, yielding a pure, unfractionated excess air component, whereas $F = 1$ means that the bubbles are not being dissolved at all. Thus, low values of F imply only slightly fractionated excess air resulting from a high degree of dissolution of the entrapped air bubbles, whereas high values of F characterize highly fractionated excess air caused by their rather incomplete dissolution.

Usually, some of the free model parameters of the CE model are well constrained in groundwater studies. For example, S is commonly negligibly low in fresh groundwater and P_{atm} is defined by the altitude of the recharge area.

The remaining unknown parameters T, A, and F can be determined from the measured Ne, Ar, Kr, and Xe concentrations using inverse techniques to solve Eq. (3) (Aeschbach-Hertig et al., 1999; Ballentine and Hall, 1999). Helium often cannot be used for this inversion because of the presence of non-atmospheric He due to the accumulation of radiogenic and terrigenic He isotopes.

In addition to the lumped-parameter models describing excess air formation as a result of the dissolution of entrapped air bubbles within the quasi-saturated zone, Mercury et al. (2004) propose a different mechanism for the formation of excess air based on increasing gas equilibrium concentrations due to increasing capillary pressure. The internal water pressure of capillary water in the unsaturated zone decreases with decreasing soil air humidity, resulting in an increase in (noble) gas equilibrium and mass fractionation in favor of the heavier noble gases. This mechanism may lead to the formation of excess air in the capillary water of very fine-grained sediments. However, capillary pressure decreases strongly with increasing soil air humidity and hence with increasing water saturation.

It is important to note that the capillary pressure model is different from the surface-tension pressure which is included in the KBD model. The latter is the result of the curvature of the bubble surface and contributes significantly to the total pressure in the bubble if the bubble radius is very small ($\lesssim$0.1 mm). In contrast, the capillary pressure model is related to the negative internal water pressure resulting from capillary forces.

3. EXPERIMENTS AND EXPERIMENTAL METHODS

Sprinkling experiments at two different field sites were conducted to study gas exchange and the formation of excess air in natural porous media. The sprinkling experiments simulated intermediate to heavy rainfall events, forcing water to infiltrate into the soil matrix. Samples of this water were taken for dissolved noble gas analysis. Commercial water sprinklers were used to distribute the water over the soil surface at the experimental field sites.

3.1. Schlüssberg site (Switzerland)

A first field experiment was conducted close to the village of Grüningen, about 20 km south-east of the city of Zürich, Switzerland. The sprinkling experiment was carried out on June 10, 2004. The experimental site (Fig. 1), which is situated on the slope of a drumlin (Schlüssberg) that was formed during the last ice age, is underlain by poorly permeable ground moraine sediments. The ground moraine is overlain by a cambisol 0.7–0.9 m thick, which has a higher hydraulic permeability due to its high macroporosity. The sediment is poorly sorted and consists of about equal proportions of clay, silt and sand (Oberrauch, 2003).

At the bottom of the slope, a trench 9 m wide and 1.6 m deep collects the lateral subsurface storm flow (Fig. 1). The upper wall of the trench is sealed with a plastic sheet to collect all lateral subsurface storm flow, which is then drained into the trench, where it can be sampled. In contrast to the Munich site (see Section 3.2), it is not possible to collect

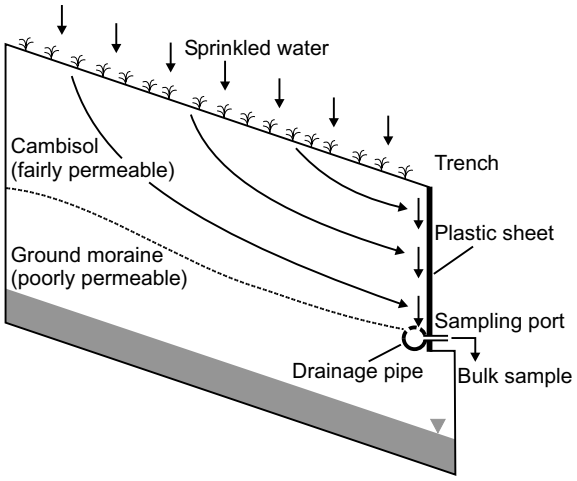

Fig. 1. Schematic experimental set-up of the Schlüssberg site. The seepage water is collected by the plastic sheet (width: 9 m, height: 1.6 m) installed vertically on the trench wall facing the slope. The water drains to the sampling port via a drainage pipe which is inclined towards the center of the trench. It is important to note that the bulk samples represent a mixture of seepage water, integrated over a width of 9 m and a depth of 1.6 m.

samples from distinct depths at the Schlüssberg site; instead, all samples represent bulk samples of the water discharging into the trench.

Water was sprinkled onto the catchment area ($\sim$110 m^2) of this trench for about 10 h at a mean rate of $\sim$10 mm/h. The lateral subsurface runoff reached 4 mm/h (Kienzler and Naef, in press). The first appearance of subsurface runoff water was observed in the trench 4 h after starting the sprinkling experiment. Subsequently, we collected samples for noble gas analysis for the next 4 h at intervals of 10–30 min.

3.2. Munich site (“Münchner Loch”, Germany)

The “Münchner Loch” is a 10 m deep research shaft situated within the unsaturated zone of the Munich Gravel Plain, an important Pleistocene aquifer located south and west of the city of Munich (Fig. 2A; Merkel et al., 1982). The sediment consists of glaciofluvial sands and sandy gravels (clay, silt: <5%, gravel: >40%) deposited during the last ice age (Kühnhardt, 1994). The thickness of the unsaturated zone is $\sim$11 m. The coarse sand-gravel aquifer has a very high hydraulic permeability of up to 10^{-2} m/s.

The accessible, circular shaft has a diameter of 1.5 m and is equipped with devices for sampling seepage water and soil air at several depths. The seepage water collectors (SWCs) are comprised of stainless steel pipes of length 50 cm and diameter 7 cm that are open on the top to receive the seepage water (Fig. 2B; Kühnhardt, 1994). Over the last 10 cm, the pipe is closed and filled with fine-grained gravel which is supported at the open part of the pipe and the outlet by screens with a mesh width of 1 mm. The SWCs are driven into the sediment and are inclined toward the shaft at an angle of 10–15°. Note that the open part of each SWC is filled with the original sediment. The outlet of the

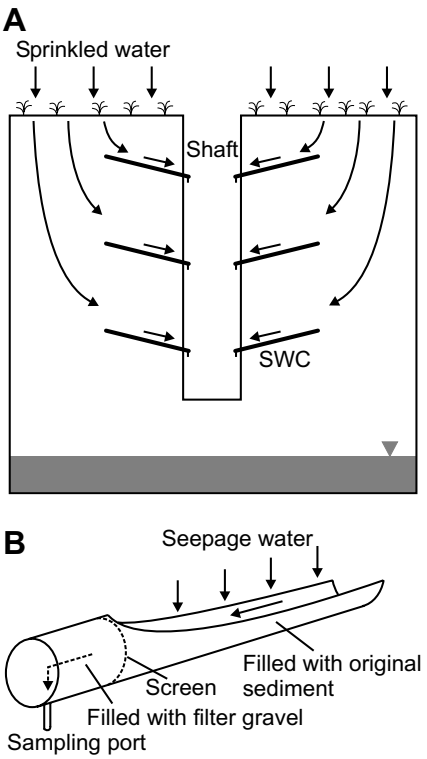

Fig. 2. (A) Schematic experimental set-up at the Munich site. Seepage water is sampled using seepage water collectors (SWC). Importantly, SWCs allow seepage water to be sampled without the need for negative pressure to suck water into the sample containers. This method therefore prevents the seepage water degassing owing to pressure reduction. (B) Design of the SWCs (length: 50 cm, diameter: 7 cm).

SWC is connected by a short silicone tube to a copper tube for noble gas sampling. In addition to water samples, soil air samples can be taken from stainless steel pipes of length 1.5 m and diameter 25 mm that are installed horizontally in the surrounding sediments.

To study the gas exchange between seepage water and soil air in the coarse sediments of the Munich Gravel Plain, we conducted two sprinkling experiments. The area adjacent to the shaft, defined as two thirds of its circumference at a distance of about 4 m, was sprinkled with water for 1.5 h (Exp. 1) and 3 h (Exp. 2) on two consecutive days (December 2 and 3, 2004). The mean water flux was about 35 mm/h. Seepage water samples for noble gas analysis were taken at depths of 0.5, 1, 2, and 3.5 m. Samples from greater depths could not be taken, because at these depths no water could be forced to flow during the experiments.

In addition to water sampling, we sampled the soil air immediately after the sprinkling experiments had been conducted. As a reference, two soil air profiles were sampled 1 month before and 3 months after the experiments.

3.3. Sampling and analytical methods

The water samples (~22.5 mL) for noble gas analysis were stored in copper tubes that can be sealed gas-tight by pinch-off clamps. Since degassing is always a critical factor during the sampling process, we exercised particular caution in order to avoid any gas loss that might have led to re-equilibration of the water during sampling.

At the Schlüssberg site, the subsurface runoff water was collected by the vertically installed plastic sheet, which drained the collected water toward the sampling port (Fig. 1). The copper tube was connected to the sampling port by a short silicone tube. Air entrapment was prevented by tapping the sample container, and the absence of air bubbles was confirmed by visual check through the silicone tube. The copper tube was pinched off after flushing several times. Because the discharge rate was high (7 L/min), the copper tube could be filled and flushed quite rapidly.

At the Munich site, seepage water collectors (SWCs) were used to collect the infiltrating water (Fig. 2). The copper tube was connected to the sampling port of the SWC using a short silicone tube. In addition to tapping the copper tube and conducting visual checks of the silicone tube, the copper tube was kept vertical in order to avoid air entrapment. The flow rate was low (a few mL/min) and sampling therefore lasted about 10–15 min per sample. The other end of the copper tube was connected to another silicone tube of about 50 cm length. The water column in this silicone tube acted as a diffusion barrier against the atmosphere and prevented (partial) re-equilibration of the water sample.

In the laboratory, the dissolved gases were extracted into an ultra-high vacuum extraction and purification line. Subsequently, the abundances of He, Ne, Ar, Kr, Xe, and the isotope ratios $^{3}He/^{4}He$, $^{20}Ne/^{22}Ne$, $^{36}Ar/^{40}Ar$ were measured using noble gas mass spectrometry in the Noble Gas Laboratory at ETH Zurich (Beyerle et al., 2000).

Samples of soil air were taken from stainless steel pipes (length 1.5 m) driven from the shaft into the sediments at different depths. The soil air samples were transferred to 500 ml stainless steel cylinders (Whitey, 304L-HDF4-500, Arbor Inc.) equipped with two plug valves (Nupro, SS-4P4T1, Arbor Inc). Samples were taken with ~3 bar overpressure using a diaphragm pump which pumped the air into the sample container. The sample container was closed after flushing the container several times with soil air. The noble gases (Ne, Ar, Kr, Xe) from the soil air samples were measured using GC–MS techniques. After passing through a drying agent (magnesium perchlorate, Merck Inc.) to remove water vapor, the air samples are injected through a 1 cm^3 gas sampling loop to the gas chromatograph (Finnigan TraceGC ultra, Thermo Inc.), and the gases are separated on a 4 m × 0.32 mm Carboxen 1010 Plot Capillary Column (Supelco Inc.) followed by a 30 m × 0.32 mm × 25 μm HP-Molsiv column. The carrier gas is He at 1.5 cm^3/min with a split ratio of 75. The oven temperature is programmed from 40 to 220 °C. The noble gases are quantified using a quadrupole mass spectrometer (Finnigan TraceDSQ, Thermo Inc.). The analytical errors deduced from the reproducibility of our air standard (dry compressed atmospheric air) are ~2% for Ne, Ar, and Kr, and ~3% for Xe. The blanks are below the detection limit for all noble gases.

4. RESULTS AND DISCUSSION

4.1. Schlüssberg site

4.1.1. Noble gases

When a water droplet from the sprinkler nozzle hits the soil surface and infiltrates into the soil, it is assumed to be in solubility equilibrium with the local atmosphere. This assumption is plausible because the water is sprinkled in the form of small drops and remains at the soil surface for several minutes as a thin water film before infiltrating. The diffusion distance z_i of noble gas i with effective diffusivity D_i can be approximated by the Einstein–Smoluchowski relation:

$$z_i = \sqrt{2D_i t} \tag{5}$$

Assuming that the water is in contact with the atmosphere for at least 10 min, and that the noble gases exhibit typical diffusivity values (Jähne et al., 1987), their diffusion distance, i.e., the characteristic length over which equilibration between water and air phases occurs, is in the range of at least several millimeters in all cases.

We applied the CE model to calculate NGTs and excess air contents. It is important to note that the aim of this work is not to verify or reject one or more of the available lumped-parameter models. We decided to use the CE model because it yields the best fit to the measured data, and because it has the most solid physical basis and extended experimental validation of all the lumped-parameter models that propose excess air formation to be the result of the dissolution of entrapped air (Kipfer et al., 2002). We did not use the capillary pressure model for two main reasons (see also further below in this section). First, the water saturation level of the subsurface zone increased to almost 100% during the sprinkling experiment (Kienzler and Naef, in press), calling into question whether the physical boundary condition for the application of the capillary pressure model, i.e., a high capillary pressure due to low relative soil air humidity, is realized at the Schlüssberg site. Second, changing mixing ratios of event and pre-event water, which were subject to different capillary pressures due to changing water saturation, do not cause any detectable change in the amount or elemental composition of the observed excess air.

The NGT reflects the temperature which prevailed during gas exchange. We used the mean NGT of (15.5 ± 1.3) °C to determine the atmospheric solubility equilibria which were established at the soil surface and during infiltration through the unsaturated zone. The mean NGT agrees with the measured temperatures of the water $(15.0 \pm 0.5$ °C) that drained into the trench during the sprinkling experiment. Thus, the gas exchange between the infiltrating water and the (soil) air is controlled by the in situ water temperature.

The noble gas concentrations in all samples from the sprinkling experiment were found to exceed significantly their respective atmospheric solubility equilibrium concentrations, which were calculated using the mean NGT (Tables 1 and 2). Values of ΔNe increase from 4% at the beginning of the experiment to 6% at the end (Fig. 3). According to the CE model, the mean entrapped air volume A is ~100 cm^3_{STP}/kg, indicating that significant amounts of air are entrapped in the soil matrix. The excess air component is found to be strongly fractionated, indicating incomplete dissolution of the entrapped gas phase. The fractionation factor F is about 0.9 for all samples, suggesting that only a few percent of the entrapped air volume is actually dissolved in the water. This is because of the small increase in pressure, and the large, available entrapped air volumes (Aeschbach-Hertig et al., 2000). Hence, the Schlüssberg experiment, as the first field experiment ever, was able to provide evidence for the formation of excess air during groundwater infiltration in a natural soil under quasi-saturated conditions.

The $^4He/^{20}Ne$ elemental ratios for all samples are slightly below the value for air-saturated water, indicating either diffusive gas loss or elemental fractionation due to multi-step equilibration (Fig. 4; Kipfer et al., 2002). However, for all samples, the values found for the $^3He/^4He$, $^{20}Ne/^{22}Ne$ and $^{36}Ar/^{40}Ar$ isotope ratios correspond closely to those found in the atmosphere, and show no fractionation within the limits of analytical error. As a result, diffusively controlled gas loss, as proposed by the partial re-equilibration model, can be excluded as a cause of the observed fractionation (Kipfer et al., 2002; Brennwald et al., 2005). The observed pattern might be caused by multi-step equilibration, i.e., the equilibration of a finite water volume with a finite gas volume, followed by the separation of the water and gas phases and the subsequent equilibration with another finite gas volume, and so forth. In this case, the secondary gas loss is controlled by the solubilities of the different gases rather than by their diffusivities. Hence, such a multi-step process, which is controlled by equilibrium partitioning governed by the Henry coefficients, would yield an elemental fractionation similar to that indicated by the measured $^4He/^{20}Ne$ ratio, but would yield no detectable isotopic fractionation for any given noble gas.

The concentrations of the heavy noble gases, especially Xe, show greater fluctuations than those of the light noble gases. These changes can be explained by a mixture of water that infiltrated during the experiment (event water) with water that was already present in the subsurface (pre-event water). If we suppose that these two types of water equilibrated at slightly different temperatures, varying mixing ratios in the water samples will affect the heavy noble gases mainly because of their strongly temperature-dependent solubilities. The same mixing would scarcely affect the light noble gas concentrations because their solubilities depend only weakly on temperature. Dye tracer tests using naphthionate which were conducted during the sprinkling experiment clearly indicate a contribution of pre-event water to the runoff (Fig. 3). Based on dye tracer concentrations, mixing ratios of pre-event and event waters in the samples can be quantified. Most of the time the fraction of pre-event water varied only slightly about a constant value, but two to three hours after the water had entered the trench, the fraction of pre-event water decreased abruptly. However, this change in the fractions of event and pre-event water was not reflected in the light noble gas concentrations (Fig. 3). The excess air component therefore seems to be

Table 1
Noble gas concentrations and isotope ratios in the water samples from the sprinkling experiments

	He (10^{-8})	Ne (10^{-7})	Ar (10^{-4})	Kr (10^{-8})	Xe (10^{-8})	R_{He}[a] (10^{-6})	R_{Ne}[b] (—)	$1/R_{Ar}$[c] (—)
				Schlüssberg				
Time (h)								
0.0	4.42	1.89	3.49	8.00	1.13	1.34	9.775	296.3
0.3	4.43	1.89	3.36	7.58	1.05	1.35	9.767	295.7
0.7	4.46	1.91	3.45	7.89	1.11	1.42	9.780	296.1
1.3	4.45	1.89	3.41	7.65	1.06	1.38	9.777	294.9
1.8	4.43	1.90	3.33	7.50	1.05	1.36	9.780	295.9
2.8	4.45	1.88	3.30	7.41	1.02	1.38	9.790	295.5
3.2	4.52	1.92	3.32	7.43	1.03	1.36	9.781	296.0
3.7	4.48	1.91	3.39	7.61	1.08	1.35	9.797	295.6
4.3	4.52	1.93	3.35	7.55	1.04	1.34	9.779	295.6
				Munich				
Depth (m)								
				Experiment 1				
0.5	4.57	2.02	4.02	9.62	1.42	1.36	9.786	296.0
1	4.51	1.96	3.92	9.36	1.41	1.42	9.803	295.8
2	4.44	1.93	3.78	8.95	1.33	1.40	9.787	295.9
3.5	4.47	1.90	3.39	7.79	1.12	1.36	9.808	294.6
				Experiment 2				
0.5	4.54	1.99	3.97	9.42	1.38	1.37	9.800	295.8
1	4.62	2.02	3.99	9.63	1.43	1.40	9.797	296.1
1	4.53	1.97	3.98	9.48	1.42	1.37	9.782	295.2
1	4.45	1.93	3.82	9.04	1.37	1.39	9.797	296.0
2	4.56	1.99	3.88	9.29	1.37	1.37	9.802	296.9
2	4.45	1.89	3.78	8.96	1.34	1.40	9.781	295.6
2	4.53	1.97	3.88	9.23	1.38	1.38	9.792	295.4
3.5	4.49	1.91	3.67	8.64	1.26	1.38	9.765	295.3
Uncertainty	0.8%	1.3%	0.5%	1.0%	1.9%	1.2%	0.2%	0.1%

All noble gas concentrations are given in cm^3_{STP}/g.
[a] $^3He/^4He$.
[b] $^{20}Ne/^{22}Ne$.
[c] $^{36}Ar/^{40}Ar$.

Table 2
NGTs and relative supersaturations in the water samples from the sprinkling experiment at the Schlüssberg site

Time (h)	NGT (°C)	ΔHe (%)	ΔNe (%)	ΔAr (%)	ΔKr (%)	ΔXe (%)
0.0	13.5 ± 3.7	2.1	3.6	7.4	7.5	8.1
0.3	15.9 ± 3.5	2.5	3.6	3.2	1.9	0.9
0.7	14.0 ± 1.7	3.0	4.5	6.2	6.1	6.8
1.3	15.5 ± 3.7	2.9	3.3	4.8	2.9	1.9
1.8	15.1 ± 0.6	2.3	3.8	2.3	0.8	0.5
2.8	16.8 ± 3.0	2.9	3.0	1.6	−0.4	−1.8
3.2	16.7 ± 1.0	4.4	4.9	2.0	−0.1	−1.3
3.7	15.0 ± 0.5	3.6	4.5	4.2	2.4	3.7
4.3	17.3 ± 2.4	4.4	5.7	2.9	1.5	−0.5
Uncertainty		0.8	1.3	1.6	2.0	2.5

independent of the occurrence and extent of the mixing of event and pre-event water, indicating that the excess air formation occurred during the sprinkling experiment in both event and pre-event water. Thus, excess air is generated in the discharging water due to hydraulic changes induced by the sprinkling experiment, i.e., by increasing water saturation, air entrapment, and partial dissolution of the air bubbles. The fact that excess air is produced in both event and pre-event waters favors the conceptual model that excess air is produced by dissolution of entrapped air – and calls into question the validity of the capillary pressure model. Because the water saturation changed due to infiltration during the sprinkling experiment, the capillary pressure also changed, and is different for pre-event and event water. However, these possible changes in capillary pressure obviously do not affect the excess air content, and hence seem not to influence the formation of excess air significantly.

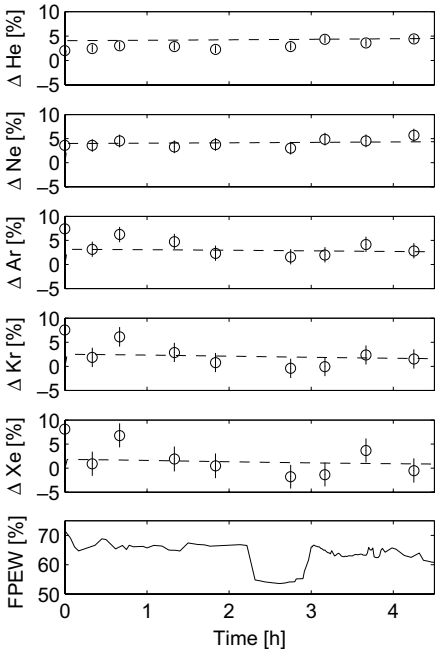

Fig. 3. Measured (circles) and modeled (dashed lines) relative supersaturations of the noble gases and the fraction of pre-event water (FPEW, solid line in the lower panel) from the sprinkling experiment at the Schlüssberg site. The error bars represent 1σ-errors.

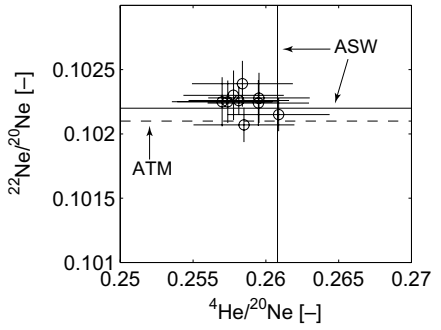

Fig. 4. Plot of ^{22}Ne/^{20}Ne against ^{4}He/^{20}Ne for the water samples from the sprinkling experiment at the Schlüssberg site (ASW—air-saturated water; ATM—atmosphere). The error bars represent 1σ-errors.

The experimental data show that a significant amount of excess air was generated during the sprinkling experiment. After sprinkling, the water infiltrated vertically along preferential flow paths. Parts of the previously unsaturated porous medium became quasi-saturated during the experiment, and lateral subsurface water flow occurred along (lateral) preferential flow paths (Fig. 5A; Kienzler and Naef, in press). The formation of the perched quasi-saturated zone is probably due to reduced hydraulic permeability at the moraine surface. Air bubbles were entrapped in the quasi-saturated sediment matrix, and the entrapped gas phase was then partially dissolved in the flowing water, which had initially been in atmospheric solubility equilibrium. A similar behavior has been observed in soil column experiments by Holocher et al. (2002). As put forward by Holocher et al. (2002, 2003), the dissolution of the entrapped gas bubbles is controlled and limited by the prevailing total pressure, and not by the amount of entrapped air available.

4.1.2. KBD model results

The sprinkling experiment was simulated using the KBD model. The parameter values defining the soil and flow characteristics of the sediment column are given in Table 3. The modeled noble gas concentrations agree reasonably well with the measured concentrations (Fig. 3).

The hydrostatic pressure corresponding to a water column of about 0.2 m (see Table 3) seems to be hardly sufficient to cause the observed supersaturations of up to 6% ΔNe. However, due to the small grain size of the sediment and the correspondingly small pore space, the entrapped air bubbles might be so small that surface-tension pressure could become relevant for the local solubility equilibrium. This is the case for bubble radii smaller than about 0.1 mm. A radius of 0.1 mm corresponds to a surface-tension pressure (P_{st}) of about 15 hPa, i.e., the surface-tension pressure is ~1.5% of the atmospheric pressure (P_{atm}). Bubble radii of about 0.01 mm ($P_{st} \approx 150$ hPa, $P_{st}/P_{atm} \approx 16\%$) to 0.05 mm ($P_{st} \approx 30$ hPa, $P_{st}/P_{atm} \approx 3\%$) would be small enough to explain the observed supersaturation without any significant hydrostatic overpressure. However, since we do not know the exact bubble radii, the contribution of the surface-tension pressure to the observed supersaturations remains speculative.

4.2. Munich site ("Münchner Loch")

4.2.1. Sprinkling experiments

Again, it is reasonable to assume that the sprinkled water is in atmospheric solubility equilibrium before it infiltrates (see Section 4.1). The noble gas concentrations measured in the seepage water from the shaft (Table 1) indicate that all samples contained little or no excess air. The ΔNe values range from −2.3% to 3.5%, and the corresponding volumes of entrapped air are very small ($< 0.35 \mathrm{cm}^3_{STP}/\mathrm{kg}$; Fig. 6, Table 4). For most of the samples, ΔNe is 0% within the limits of analytical error. In all samples, the heavy noble gases are in atmospheric solubility equilibrium. Further, there is no significant relationship between the amount of excess air and either sampling depth or sampling time.

The fact that the samples contain virtually no excess air suggests that gas exchange between seepage water and soil air occurred at atmospheric pressure or at only marginally enhanced pressure. Further, the almost complete absence of detectable excess air indicates that hardly any air was entrapped in the quasi-saturated zone of the soil matrix during the infiltration experiment, and that capillary pressures are negligibly small, as would be expected in coarse sediments.

The atmospheric solubility equilibria are mainly controlled by the temperature prevailing during gas exchange, which is reflected in the NGT. Remarkably, the NGT exhibits a continuous significant increase with depth (Fig. 7, Table 4). Usually, the NGT is assumed to correspond to the mean annual soil temperature (Stute and

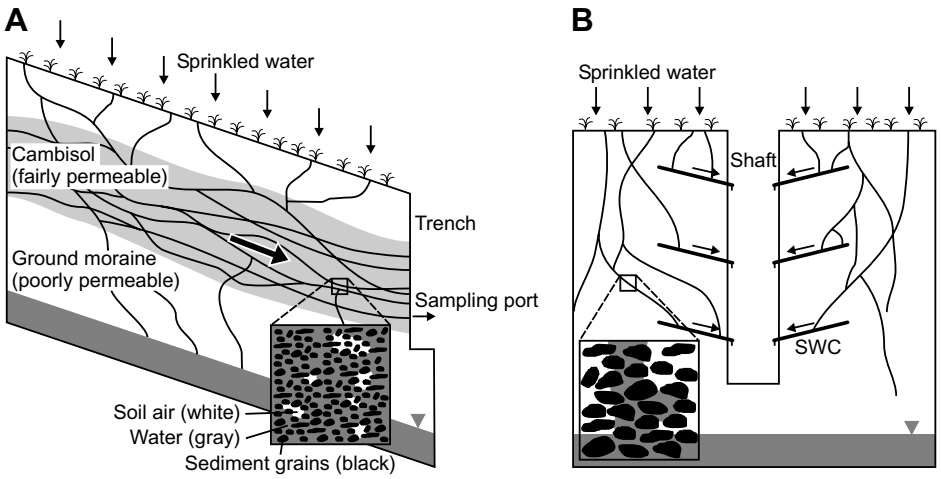

Fig. 5. Schematic cross sections showing the conceptual models of the sprinkling experiments at the Schlüssberg and Munich sites. At the Schlüssberg site (A), the sprinkled water infiltrates into the soil and lateral subsurface flow is generated by partial saturation of the fine-grained unsaturated zone due to the reduced hydraulic permeability at the moraine surface. Vertical and lateral flow occurs along preferential flow paths (Kienzler and Naef, in press). Air is entrapped in the quasi-saturated zone and partly dissolved due to the increased hydrostatic (and surface-tension) pressure. In contrast, during the sprinkling experiment in Munich (B), the water infiltrates along preferential flow paths into the seepage water collectors (SWC) without saturating large zones of the coarse soil. Soil air is still in contact with the free atmosphere, and gas exchange between the soil air and the infiltrating water is controlled by atmospheric pressure. Therefore, hardly any excess air is generated in the infiltrating water.

Table 3
Model parameters for the KBD simulation of the Schlüssberg experiment

Model parameter	Value	Parameter estimation
Column length	0.2 m	Best fit to measured data
Initial bubble radius	0.1 mm	Rough estimate from mean grain size
Total porosity	0.4	Typical value of fine-grained sand and silt deposits
Air–water ratio	0.1	Estimated from CE model results
Water temperature	15.5 °C	Mean NGT
Atmospheric pressure	954.6 hPa	Estimated from measurements at meteorological stations close to the study site
Salinity	0 ‰	Fresh water
Filter velocity	8×10^{-6} m/s	Estimated from volume of sprinkling water applied
Dispersion coefficient	8×10^{-7} m^2/s	Estimated from filter velocity, assuming a dispersivity of 0.1 m
Initial noble gas concentrations	C_i^{equ}	The water from the sprinklers is in atmospheric solubility equilibrium before infiltration (see Section 4.1)

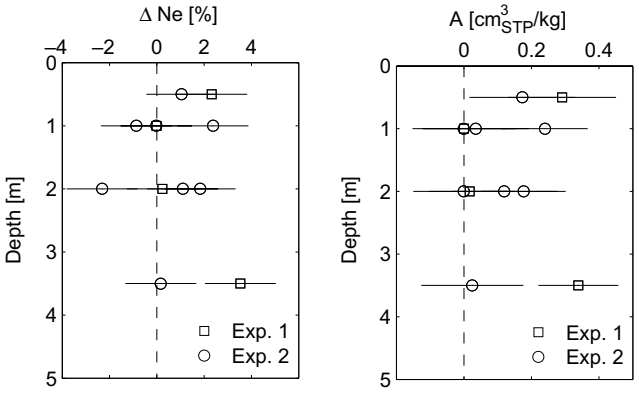

Fig. 6. Depth profiles of ΔNe and dissolved excess air volumes (A) resulting from the sprinkling experiments (Exp. 1 and Exp. 2) in Munich. The error bars represent 1σ-errors.

Table 4
ΔNe, excess air (A), and NGTs of the water samples from the sprinkling experiments in Munich

Depth (m)	ΔNe (%)	A (cm^3_{STP}/g)	NGT (°C)
	Experiment 1		
0.5	2.3	0.29	6.0
1	0.0	0.00	6.7
2	0.2	0.02	8.2
3.5	3.5	0.34	13.3
	Experiment 2		
0.5	1.1	0.17	6.7
1	2.4	0.24	6.3
1	0.0	0.04	6.4
1	−0.9	0.00	7.9
2	1.8	0.18	7.5
2	−2.3	0.00	8.3
2	1.1	0.12	7.5
3.5	0.2	0.02	9.7
Uncertainty	1.5	0.14	0.2

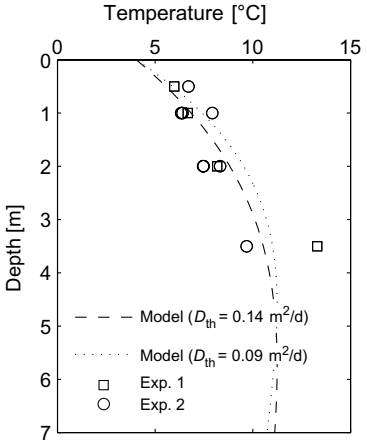

Fig. 7. Comparison of NGTs (circles/squares) and modeled soil temperatures (dashed/dotted lines) based on two different values of thermal diffusivity (D_{th}) resulting from the sprinkling experiments (Exp. 1 and Exp. 2) in Munich. All samples – with one exception (Exp. 1, depth: 3.5 m) which gives an unrealistically high NGT – agree with the modeled soil temperature profile for the date of sampling. All errors of the NGTs are 0.2 °C.

Sonntag, 1992; Stute and Schlosser, 1993). The application of noble gases as a paleothermometer depends crucially on this basic assumption. Unfortunately, direct measurements of soil temperature at the study site were not available. We therefore applied a soil temperature model to reconstruct the local soil temperature at the field site as a function of soil depth and time.

The soil temperature profile can be described by the following partial differential "thermal conduction" equation (e.g., Hillel, 2003):

$$\frac{\partial T(z,t)}{\partial t} = D_{th}\frac{\partial^2 T(z,t)}{\partial z^2} \tag{6}$$

with D_{th} being the thermal diffusivity. Eq. (6) is solved for the following boundary conditions:

1. At the soil surface ($z = 0$) an annual sinusoidal temperature variation is assumed around the annual mean soil temperature T_a:

$$T(0,t) = T_a + A_0 \sin\left(\frac{2\pi(t-t_0)}{365} - \frac{\pi}{2}\right) \tag{7}$$

   A_0 is the annual amplitude of the surface soil temperature and t_0 is the time lag from an arbitrary starting date (taken as January 1 here) to the time of occurrence of the annual minimum.
2. As $z \to \infty$ the soil temperature tends to the (constant) annual mean soil temperature. The geothermal heat flux is negligible in comparison with the exchange fluxes to and from the atmosphere.
3. The thermal diffusivity D_{th} is constant throughout the soil profile and throughout the year.

The resulting temperature model is described by the following sinusoidal function:

$$T(z,t) = T_a + A_0 \exp(-z/d)\cdot \sin\left(\frac{2\pi(t-t_0)}{365} - \frac{z}{d} - \frac{\pi}{2}\right) \tag{8}$$

with damping depth $d = (2D_{th}/\omega)^{1/2}$ and angular frequency $\omega = 2\pi/365\ d^{-1}$. The parameter values $T_a = 9.65 \pm 0.03$ °C, $A_0 = 9.38 \pm 0.07$ °C, $t_0 = 24.0 \pm 0.4$ d, and $D_{th} = 0.09 \pm 0.01\ m^2\ d^{-1}$ were determined from time series of daily mean soil temperatures measured at 0.05, 0.20, and 0.50 m depths in 2004. The soil temperature measurements were performed at the Roggenstein meteorological station about 20 km north-west of the study site (data are available at http://www.lfl.bayern.de, Bayerische Landesanstalt für Landwirtschaft). The climatic characteristics of the station are similar to those of our study site. Since the thermal diffusivity D_{th} depends on local soil properties, we also determined D_{th} from older soil temperature measurements at our study site. The value $D_{th} = 0.14 \pm 0.03\ m^2\ d^{-1}$ was obtained from a calibration based on soil temperature measurements from the shaft at depths of 0.2–9 m (data given in Freitag et al., 1987). The climate-related parameters T_a, A_0, and t_0 were calculated from more recent data that comprise temperature measurements from the year in which the sprinkling experiments were performed. We employed the Gauss-Newton method to determine the parameters.

Fig. 8 shows the comparison of the measured and simulated soil temperatures for the Roggenstein station. The model reproduces the measured values well, and can therefore be assumed to be adequate to calculate the soil temperature profile at our study site. The NGTs determined from concentrations of noble gases in the seepage water agree fairly well with the modeled soil temperature depth profile (Fig. 7).

The infiltration of pre-event water, which would have equilibrated under different temperatures prior to the experiment, could offer a further possible explanation for the observed increase in NGTs with depth if pre-event water formed larger perched saturated zones that prevented the water from re-equilibration with soil air. However, there

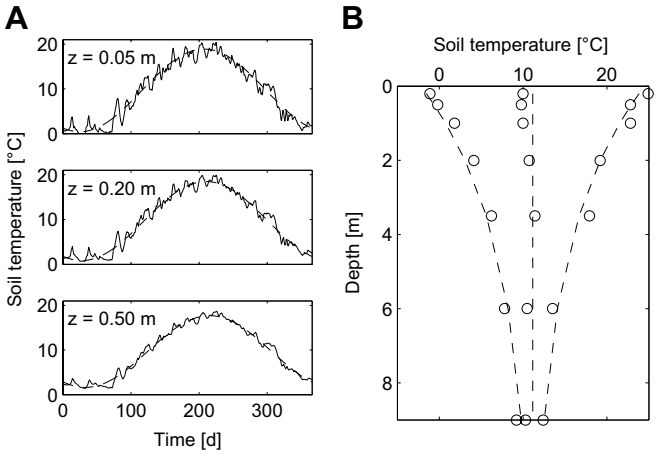

Fig. 8. (A) Comparison of measured (solid lines), and modeled (dashed lines) soil temperatures at three different depths z at the Roggenstein station in 2004. The modeled soil temperatures were obtained by applying the thermal conduction Eq. (6). (B) Measured (circles) and modeled (dashed lines) soil temperatures at the Munich site. The circles represent minimum, maximum, and mean values of 1000 soil temperature measurements conducted during the 1980s.

are two reasons to doubt the validity of this hypothesis. (i) The $^3He/^4He$ ratios do not indicate any significant accumulation of tritiogenic ^3He, excluding the presence of water with residence times of several months. (ii) As is known from previous studies at the same site (Freitag et al., 1987), the soil water content is about 5–10%. This is owing to the small field capacity and the high hydraulic permeability of the coarse sediments. Therefore, the formation of larger perched saturated zones which prevent gas exchange between water and the local soil air is unlikely.

Thus, we conclude that the NGTs indeed reflect the soil temperature of the unsaturated zone, and that the water from the sprinkling experiments, which is assumed to have infiltrated along preferential flow paths, continuously exchanged gases with the soil air under atmospheric pressure conditions. In contrast to the Schlüssberg field site, a quasi-saturated zone did not form during infiltration, and no significant entrapment of air bubbles occurred (Fig. 5B).

4.2.2. Soil air

In addition to analyzing samples of seepage water, we measured the composition of gases in samples of soil air. Application of excess air models implies that the concentrations of the noble gases in soil air are identical to those in atmospheric air. The soil air samples were analyzed in order to verify this assumption. Samples were taken at depths of 1, 3.5, 6, and 9 m. The measurements show that the noble gas concentrations at all depths indeed correspond to those of free atmospheric air (Fig. 9). In addition, no significant differences could be observed between the profile sampled immediately after the sprinkling experiments and the reference profiles. The assumption that the

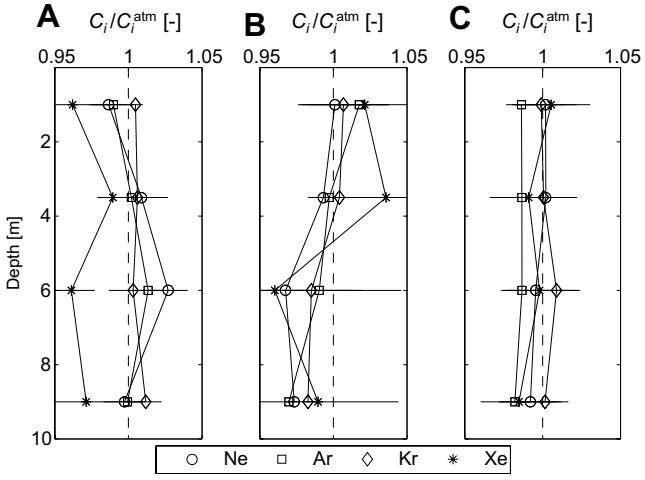

Fig. 9. Noble gases in the soil air at the Munich site (A: November 3, 2004; B: December 3, 2004; C: March 7, 2005). All noble gas concentrations (C_i) are normalized to the relevant atmospheric concentrations (C_i^{atm}). Profile B was sampled immediately after the sprinkling experiments. The error bars represent 1σ-errors.

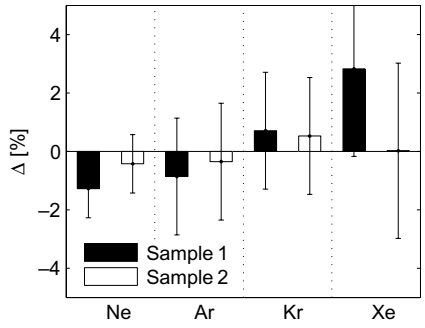

Fig. 10. Relative saturations of the noble gases dissolved in the groundwater samples at the Munich site with respect to their respective atmospheric solubility equilibria. Both samples are in atmospheric solubility equilibrium within analytical uncertainty. The error bars represent 1σ-errors.

concentrations of the noble gases Ne, Ar, Kr, and Xe in the soil air are equivalent to those in atmospheric air is therefore appropriate.

4.2.3. Groundwater

Additionally, we obtained two samples of shallow groundwater from an observation well situated close to the shaft. The noble gas concentrations in both samples were in atmospheric solubility equilibrium (Fig. 10). The groundwater samples therefore support the findings gained from the sprinkling experiments. Hence, both lines of evidence suggest that little or no excess air is produced during infiltration into the local aquifer system.

5. CONCLUSIONS

The results of the sprinkling experiments at the Schlüssberg and Munich sites add further evidence supporting the hypothesis that the formation of excess air depends on the infiltration mechanism and soil characteristics.

The fine-grained sediments of the Schlüssberg field site were partly saturated during the sprinkling experiment, forming perched water lenses due to the reduced hydraulic permeability at the moraine surface. Air bubbles were entrapped in the soil matrix by the infiltrating water (Fig. 5A). The captured air bubbles were partly dissolved in the surrounding water, producing excess air owing to an increase in pressure – probably in both hydrostatic and surface-tension pressures – with respect to the free atmosphere. The strongly fractionated excess air component in the water samples indicates the presence of large volumes of entrapped air which were dissolved in the water only to a small extent.

By contrast, the results from the Munich experiment show that virtually no air could be entrapped by the water infiltrating into the highly permeable, coarse sands and gravels (Fig. 5B), and that noble gas concentrations were in local equilibrium with free soil air. The absence of excess air in the infiltrating water suggests that the soil air was connected to the free atmosphere, and that gas exchange occurred at atmospheric pressure rather than at increased hydrostatic pressure between a finite entrapped air volume and the surrounding water phase, as was observed at the Schlüssberg site. There are no small pores in the coarse gravel that would allow the capillary pressure to become relevant for the solubility equilibrium.

Importantly, the NGTs, which increase with depth, clearly indicate the occurrence of gas exchange between the infiltrating water and the soil air, with the dissolved noble gas concentrations reaching equilibrium at atmospheric pressure conditions and reflecting the in situ soil temperature. This finding is of significant importance for the use of dissolved atmospheric noble gases as a proxy for paleotemperatures, as it provides an experimental evidence supporting the assumption that NGTs are identical to (past) soil temperatures.

The field experiments conducted imply the existence of a strong functional dependence of both gas exchange and excess air formation on soil properties during the infiltration process. However, infiltration dynamics could also have a significant impact on the formation of excess air. For example, the influence of the infiltration rate – normalized to the hydraulic properties of the sediments – should therefore be assessed in future studies.

This study has focused on gas exchange and the formation of excess air during the infiltration process within the unsaturated zone. However, excess air can also be formed as a result of air being trapped by a rise in the groundwater table, caused either by local infiltration or by pressure transmission. Furthermore, other aspects of gas/water partitioning in porous media which play only a minor role in the current study – e.g., the role of capillary pressure in the unsaturated zone (see Mercury et al., 2004) – still remain unexplained and would require further field experiments to be conducted.

ACKNOWLEDGMENTS

We would like to thank Christian Holzner and Helena Amaral for their help during the field work in Munich, and Markus Hofer and Nora Graser for analyzing the soil air samples. Thanks are also due to Associate Editor Bernard Marty, Axel Suckow, Chris Ballentine, and an anonymous reviewer for their valuable and constructive reviews which helped to improve our manuscript. This work was supported by the Swiss National Science Foundation (Project No. 200020-107489/1).

REFERENCES

Aeschbach-Hertig W., Peeters F., Beyerle U., and Kipfer R. (1999) Interpretation of dissolved atmospheric noble gases in natural waters. *Water Resour. Res.* **35**(9), 2779–2792.

Aeschbach-Hertig W., Peeters F., Beyerle U., and Kipfer R. (2000) Palaeotemperature reconstruction from noble gases in ground water taking into account equilibration with entrapped air. *Nature* **405**, 1040–1044.

Ballentine C. J., and Hall C. M. (1999) Determining paleotemperature and other variables by using an error-weighted, nonlinear inversion of noble gas concentrations in water. *Geochim. Cosmochim. Acta* **63**(16), 2315–2336.

Beyerle U., Purtschert R., Aeschbach-Hertig W., Imboden D. M., Loosli H. H., Wieler R., and Kipfer R. (1998) Climate and groundwater recharge during the last glaciation in an ice-covered region. *Science* **282**, 731–734.

Beyerle U., Aeschbach-Hertig W., Peeters F., Kipfer R., Purtschert R., Lehmann B., Loosli H., and Love A. (1999) Noble gas data from the Great Artesian Basin provide a temperature record of Australia on time scales of 10^5 years. In: Isotope techniques in water resources development and management, IAEA-SM-361/25, pp. 57–58. IAEA, Vienna.

Beyerle U., Aeschbach-Hertig W., Imboden D. M., Baur H., Graf T., and Kipfer R. (2000) A mass spectrometric system for the analysis of noble gases and tritium from water samples. *Environ. Sci. Technol.* **34**(10), 2042–2050.

Beyerle U., Redi J., Leuenberger M., Aeschbach-Hertig W., Peeters R., Kipfer R., and Dodo A. (2003) Evidence for periods of wetter and cooler climate in the Sahel between 6 and 40 kyr BP derived from groundwater. *Geophys. Res. Lett.* **30**(4), 1173.

Brennwald M. S., Imboden D. M., and Kipfer R. (2005) Release of gas bubbles from lake sediment traced by noble gas isotopes in the sediment pore water. *Earth Planet. Sci. Lett.* **235**(1–2), 31–44.

Clever H. L. (ed.) (1979) *Krypton, Xenon and Radon-gas Solubilities, Solubility Data Series*, vol. 2. Pergamon Press, Oxford.

Cook P. G., and Herczeg A. L. (2000) *Environmental Tracers in Subsurface Hydrology*. Kluwer Academic Publishers, Boston.

Freitag G., Großmann J., Hoffmann M., Merkel B., Prömper R., Sperling B., Udluft P., and Ullsperger I. (1987) Beschaffenheit und Abfluss von Sickerwässern aus einem städtischen Siedlungsgebiet. Tech. rep., TU München.

Heaton T. H. E., and Vogel J. C. (1981) "Excess air" in groundwater. *J. Hydrol.* **50**, 201–216.

Hillel D. (2003) *Introduction to Environmental Soil Physics*. Elsevier, Amsterdam.

Holocher J., Peeters F., Aeschbach-Hertig W., Hofer M., Brennwald M., Kinzelbach W., and Kipfer R. (2002) Experimental investigations on the formation of excess air in quasi-saturated porous media. *Geochim. Cosmochim. Acta* **66**(23), 4103–4117.

Holocher J., Peeters F., Aeschbach-Hertig W., Kinzelbach W., and Kipfer R. (2003) Kinetic model of gas bubble dissolution in groundwater and its implications for the dissolved gas composition. *Environ. Sci. Technol.* **37**(7), 1337–1343.

Jähne B., Heinz G., and Dietrich W. (1987) Measurement of the diffusion coefficients of sparingly soluble gases in water. *J. Geophys. Res.* **92**(C10), 10767–10776.

Kienzler P., and Naef F. (in press) Subsurface storm flow formation at different hillslopes and implications for the "old water paradox". *Hydrol. Process*.

Kipfer R., Aeschbach-Hertig W., Peeters F., and Stute M. (2002) Noble gases in lakes and ground waters. In: *Noble Gases in Geochemistry and Cosmochemistry*, vol. 47 of *Rev. Mineral. Geochem.* (eds. D. Porcelli, C. Ballentine, and R. Wieler), pp. 615–700. Mineralogical Society of America, Geochemical Society.

Kühnhardt M. (1994) Untersuchungen zur Dispersion von polyzyklischen aromatischen Kohlenwasserstoffen (PAHs) in der ungesättigten Zone eines fluvioglazialen Schotters. PhD thesis, TU München.

Mazor E. (1972) Paleotemperatures and other hydrological parameters deduced from gases dissolved in groundwaters, Jordan Rift Valley, Israel. *Geochim. Cosmochim. Acta* **36**(12), 1321–1336.

Mercury L., Pinti D. L., and Zeyen H. (2004) The effect of the negative pressure of capillary water on atmospheric noble gas solubility in ground water and palaeotemperature reconstruction. *Earth Planet. Sci. Lett.* **223**, 147–161.

Merkel B., Nemeth G., Udluft P., and Grimmeisen W. (1982) Hydrogeologische und hydrochemische Untersuchungen in der ungesättigten Zone eines Kiesgrundwasserleiters. Teil 1: Entwicklung und Erstellung eines begehbaren Probenahmeschachtes zur Boden-, Wasser- und Luftuntersuchung. *Z. Wasser-Abwasser-Forsch.* **15**, 191–195.

Oana S. (1957) Bestimmung von Argon in besonderem Hinblick auf gelöste Gase in natürlichen Gewässern. *J. Earth Sci. Nagoya Univ.* **5**, 103–124.

Oberrauch F. (2003) Experimentelle Quantifizierung von Pre-Event Water. Diploma thesis, Universität für Bodenkultur, Vienna.

Schwarzenbach R. P., Gschwend P. M., and Imboden D. M. (2003) *Environmental Organic Chemistry*, 2nd ed. John Wiley and Sons, New York.

Stute M., and Schlosser P. (1993) Principles and applications of the noble gas paleothermometer. In: *Climate Change in Continental Isotopic Records, of AGU Geophysical Monograph Series*, (eds. P.K. Swart, K.C. Lohmann, J. McKenzie and S. Savin), pp. 89–100. American Geophysical Union, Washington, DC.

Stute M., and Sonntag C. (1992) Paleotemperatures derived from noble gases dissolved in groundwater and in relation to soil temperature. In: *Isotopes of noble gases as tracers in environmental studies*, pp. 111–122. IAEA, Vienna.

Stute M., Clark J., Schlosser P., and Broecker W. (1995a) A 30,000 yr continental paleotemperature record derived from noble gases dissolved in groundwater from the San Juan Basin, New Mexico. *Quaternary Res.* **43**, 209–220.

Stute M., Forster M., Frischkorn H., Serejo A., Clark J. F., Schlosser P., Broecker W. S., and Bonani G. (1995b) Cooling of tropical Brazil (5 °C) during the Last Glacial Maximum. *Science* **269**, 379–383.

Weiss R. F. (1970) The solubility of nitrogen, oxygen and argon in water and seawater. *Deep-Sea Res.* **17**(4), 721–735.

Weiss R. F. (1971) Solubility of helium and neon in water and seawater. *J. Chem. Eng. Data* **16**(2), 235–241.

Weiss R. F., and Kyser T. K. (1978) Solubility of krypton in water and seawater. *J. Chem. Eng. Data* **23**(1), 69–72.

Wilson G. B., and McNeill G. W. (1997) Noble gas recharge temperatures and the excess air component. *Appl. Geochem.* **12**(6), 747–762.

Associate editor: Bernard Marty